Detection of oil in and under ice

W. Scott Pegau[1], Jessica Garron[2], Leonard Zabilansky[3], Christopher Bassett[4], Job Bello[5], John Bradford[6], Regina Carns[7], Zoe Courville[3], Hajo Eicken[2], Bruce Elder[3], Peter Eriksen[8], Andone Lavery[9], Bonnie Light[7], Ted Maksym[9], Hans-Peter Marshall[6], Marc Oggier[2], Don Perovich[3], Pawel Pacwiardowski[8], Hanumant Singh[9], Dajun Tang[7], Chris Wiggins[10], Jeremy Wilkinson[11]

[1]Oil Spill Recovery Institute, Box 705 Cordova, AK 99574

[2]University of Alaska Fairbanks, Box 757340 Fairbanks, AK 99775

[3]Cold Regions Research and Engineering Laboratory, 72 Lyme Road, Hanover, NH 03755

[4]NOAA Northwest Fisheries Science Center, 2725 Montlake Blvd East, Seattle WA 98112

[5]EIC Laboratories, 111 Downey St. Norwood, MA 02062

[6]Boise State University 1910 W. Unversity Dr. Boise, ID 83725

[7]University of Washington 1013 NE 40th St, Seattle, WA 98105

[8]Norbit US, 325 Oak View Ln, Santa Barbara, CA 93111

[9]Woods Hole Oceanographic Institution, 86 Water St, Woods Hole, MA 02543

[10]Inland Gulf Maritime 3496 Halls Mill Rd, Mobile, AL 36693

[11]Polar Ocean Services, Tullich, Taynuilt, Scotland, PA35 H1Y

ABSTRACT (2017-147)

In 2014, researchers from ten organizations came to the U.S. Army Corps of Engineers, Cold Regions Research and Engineering Laboratory (CRREL) in New Hampshire to conduct a first of its kind large-scale experiment aimed at determining current sensor capabilities for detecting oil in and under sea ice. This project was the second phase of the Oil Spill Detection in Low Visibility and Ice research project of the International Association of Oil and Gas Producers (IOGP), Arctic Oil Spill Response Technology - Joint Industry Programme.

The objectives of the project were to:

- Acquire acoustic, thermal, optical and radar signatures of oil on, within, and underneath a level sheet of laboratory sea ice.
- Determine the capabilities of various sensors to detect oil in specific ice environments created in a test tank, including freeze-up, growth and melt.
- Model the potential performance of the sensors under realistic field conditions using the test data for validation.
- Recommend the most effective sensor suite of existing sensors for detecting oil in the ice environment.

The sensor testing spanned a two-month ice growth phase and a one-month decay/melt period. The growth phase produced an 80 centimeter thick level sheet of salt water ice representative of natural sea ice grown under quiescent conditions.

Above-ice sensors included frequency modulated continuous wave radar, ground penetrating radar, laser fluorescence polarization sensor, spectral radiometer, visible and infrared cameras.

Below-ice sensors included acoustics (broadband, narrowband, and multibeam sonars), spectral radiometers, cameras, and fluorescence polarization. Measurements of physical and electrical properties of the ice and oil within the ice were provided to optical, acoustic, and radar modelers as inputs into their models. The models were then used to extrapolate the sensors' laboratory performance to potential performance over a range of field conditions.

All selected sensors detected oil under some conditions. The radar systems were the only above-ice sensors capable of detecting oil below or trapped within the ice. Cameras below the ice detected oil at all stages of ice growth, and the acoustic and fluorescence systems detected encapsulated oil through limited amounts of new ice growth beneath the oil.

No single sensor detected oil in and below ice under all conditions tested. However, we used the test results to identify suites of sensors that could be deployed today both above and below the ice to detect and map an oil spill within ice covered waters.

INTRODUCTION

Increased interest in the potential for oil and gas exploration and development in the Arctic, coupled with increasingly ice-free waters and expected subsequent increases in shipping activity (Eguiluz et al., 2016), highlights the need to develop technologies that allow effective response to an oil spill in ice-covered waters. One challenge to responding in the Arctic is to be able to detect and track oil in the extreme environmental conditions often encountered. Safely mapping spilled oil throughout the year, in open-water as well as the various ice-covered water scenarios and within a wide range of visibility conditions, is an essential component of spill response in the Arctic.

Innovative remote sensing systems and platforms proposed for surveying both above and below the ice have the potential improve our ability to detect oil and to reduce human risk in oil spill response activities (Bradford et al., 2008; Brown, 2011; Dickins et al., 2012; Fingas & Brown, 2013; Puestow et al., 2013; Wilkinson et al. 2013; Maksym et al., 2014 and others). Advances in the capabilities of autonomous underwater vehicles and unmanned aircraft systems are leading to new platforms that can carry a range of sensors more safely over longer distances. What remains to be demonstrated are the capabilities of individual sensors to detect oil under a range of ice conditions in an Arctic field environment. Previous research has shown that no single sensor can cover all ice conditions (Dickins et al., 2010); therefore, it is important to understand the advantages and limitations to each sensor, as well as to identify a suite of sensors that maximize the range of conditions in which oil can be detected.

In January 2012, the oil and gas industry launched a collaborative effort to enhance Arctic oil spill capabilities under the auspices of the International Association of Oil and Gas Producers (IOGP). This collaboration, called the Arctic Oil Spill Response Technology Joint Industry Programme (JIP) was designed to expand Arctic oil spill response capabilities. Six key areas of research were identified for further experimentation and study: dispersants, environmental effects, trajectory modelling, remote sensing (oil spill detection and mapping in low visibility and ice), mechanical recovery and in situ burning. To address the objectives associated with remote sensing, the JIP sponsored an evaluation of existing remote sensing technologies (Puestow et al., 2013, Wilkinson et al., 2013) followed by a large-scale laboratory experiment to test the capabilities of the most promising sensors.

The laboratory based sensor testing began in November 2014 and spanned a two-month ice growth phase and a one-month decay/melt period. The test basin ice was representative of

natural level sea ice grown under quiescent conditions, creating a controlled baseline environment to compare different sensors with a manageable number of variables. Eight above-ice systems and eleven below-ice systems were used to collect measurements of oil properties through various thicknesses of ice. Modeling was used to extrapolate the sensor's laboratory performance to field conditions in flat first-year ice. Described here are the results of laboratory testing to determine the ability of various existing technologies to detect oil in, on, and under ice. The purpose of this paper is to provide an overview of the experiment and its findings; a more detailed description of the work and results can be found in the project's final report to the JIP (Pegau et al., 2016).

METHODS

Testing was conducted in the Test Basin in the Ice Engineering Facility at the US Army Corps of Engineers Cold Regions Research and Engineering Laboratory (CRREL) in Hanover, New Hampshire. The tank was filled and salt (NaCl) added to reach a starting salinity of 27 PSU. Over a two month period, an 80-centimeter thick sheet of level, salt-water ice was grown. Following the growth phase, the basin was allowed to slowly warm and observations collected through a month long decay phase.

The surface area of the basin (37 m x 9 m, water depth 2.4 m) was subdivided into test areas using rectangular confinement hoops (Fig. 1). Hoops were fabricated using PVC pipes with a vertical hanging polyester curtain. The curtains in Hoop 2-5 were trimmed so they extended 15 cm below the anticipated ice thickness when the oil injection occurred to avoid oil migration beyond the curtain and to reduce the interference from the curtains on measurements. The primary hoops were placed along the centerline of the tank to allow both the submerged and

surface sensors to monitor the same areas. These centerline hoops were 3m long by 2.5m wide except for Hoop 1, which was 3m long by 6m wide. The wider Hoop 1 was designed to evaluate the side looking capability of the multi-beam sensor. To preserve the ice structure in the primary hoops, secondary hoops designated with "A" suffix received the same oil treatment as the corresponding primary hoops. Special purpose hoops designated with a "B" suffix were placed off center and used for specialized experiments using a portion of the sensors. A large area of ice along the south side of the basin was left clear to provide a space to remove ice cores during the experiment.

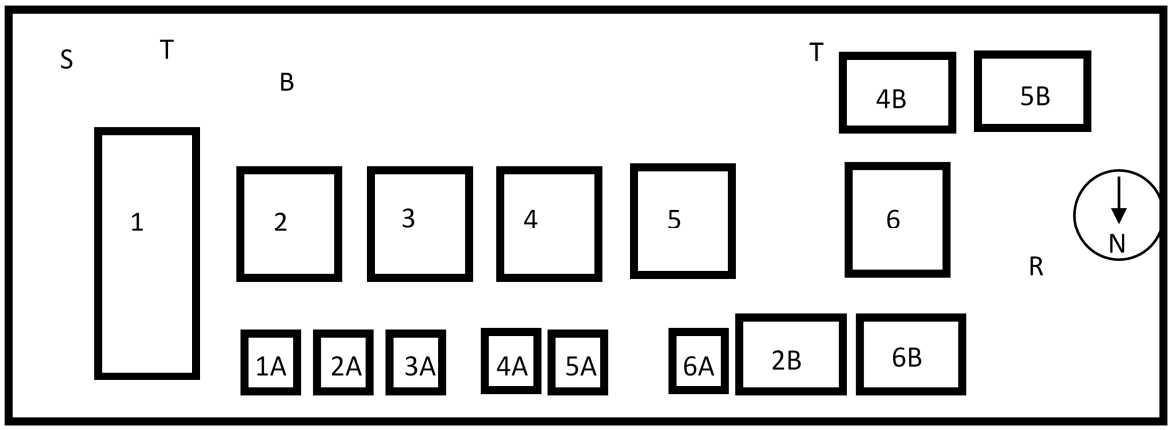

Figure 1. The conceptual layout of the experiments. Ancillary sensors include, thermistor strings (T), resistivity measurements (R), ice sound speed (S), and rotating broadband sonar (B).

Suites of above-ice and below-ice sensors were deployed on carriages that ran the full length of the tank along the central axis. Above-ice sensors were mounted on a 5 m long boom attached to the carriage 2 m above the ice (Fig. 2) and included:

- Frequency modulated continuous wave (FMCW) radar,
- Ground penetrating radars (GPR),

- Visible and thermal infrared (IR) cameras,
- Laser fluorescence polarization (FP) sensor.

The FMCW was a custom built radar transmitting and receiving a single polarization with a frequency sweep from 0.5 to 2 GHz. The GPRs were Pulse EKKO Pro 0.5 GHZ dual polarization and a 1.5 GHZ unit. A BAE combined visible and IR camera was used along with a GoPro camera. The fluorosensor was an EIC Lab system with a 405 nm laser with a phase locked detector system designed to measure fluorescence a distance from the sensor. Additionally, GPR (0.5 and 1.0 GHz), thermal infrared (IR), and visible and near-infrared spectral albedo (ASD Fieldspec Pro, 350-2500 nm) measurements were collected at the ice surface.

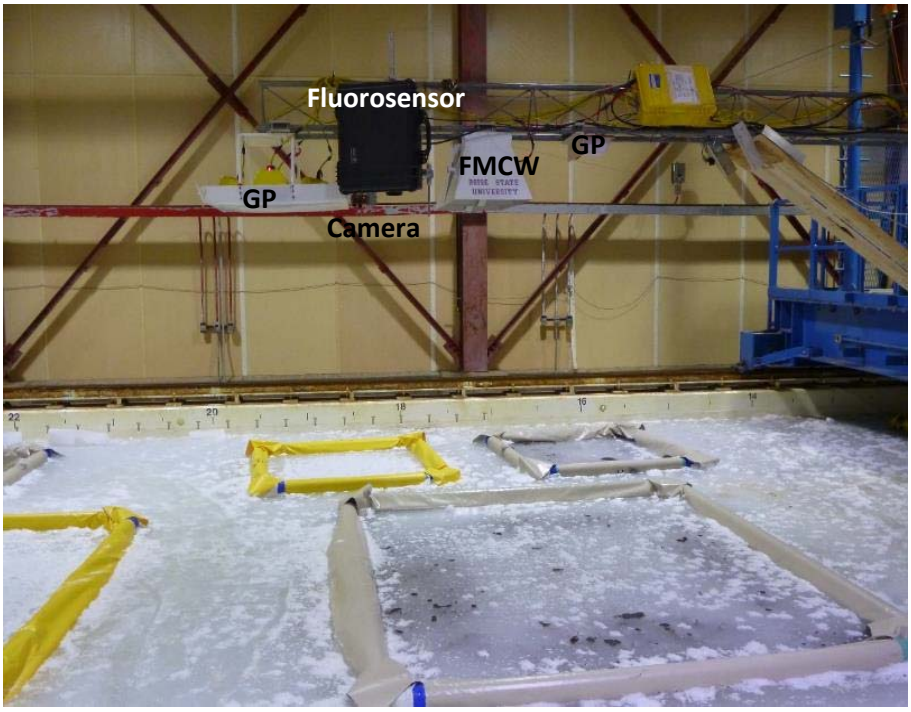

Figure 2. The aerial sensors mounted on the boom.

Below-ice sensors were mounted on a trolley running on rails on the tank floor 2.4 m below the water surface (Fig. 3), and included:

- Spectral radiance and irradiance sensors,
- Laser fluorescence polarization FP sensors,
- Optical cameras,
- Broadband acoustics,
- Narrowband acoustics,
- Multibeam acoustics.

The radiance and irradiance sensors were manufactured by Trios and measured the transmitted light from 320 to 950 nm with 3.3 nm resolution. The fluorescence sensor was an EIC lab scanning fluorometer with 405 nm excitation and a focal plane set at the base of the ice. Cameras included a pair of low-light black and white cameras and a pan-tilt-zoom color camera. The broadband acoustics were built on a modified Edgetech 2200 with transmission frequency bandwidths of 75-130, 115-225, and 370-590 kHz. Two sets of transducers were used ,with one set looking in the nadir direction and the other mounted 20 degrees off nadir. The narrowbeam sonar was an Aquascat 1000 unit transmitting at 0.3, 0.5, 1, and 5 MHz. Upward looking Norbit multibeam units transmitted at 200 and 400 kHz with an 80 kHz bandwidth and a forward looking unit transmitted at 400 kHz.

Figure 3. Top left, the rail system with the chain between the rails run down the center of the tank. Fixed sensors can be seen on the right side of the image. Top right, the sensor plate mounted to the carriage underwater. (A) The servo motor, (B) CRREL camera system on the carriage, and (C) the instrument plate. Bottom, The instrument plate out of the water. (D) Trios spectral radiance and irradiance sensors, (E) EIC Labs scanning laser fluorosensor, (F) broadband acoustic transceivers, (G) narrow band acoustic transceivers, (H) low light camera, (I) light source for the cameras, (J) Norbit 400 kHz multibeam sonar, (K) Norbit 200 kHz multibeam sonar, (L) Norbit FLS.

During the growth phase the basin room temperature was brought down and held near -24°C. At predetermined ice thicknesses Alaska North Slope crude oil at 0°C was injected under the ice into the respective experimental hoops. Within two days following an oil injection, ice would begin to form below the oil. The ice below the oil continued to grow, encapsulating the oil and providing ice thicknesses below the oil ranging from 0 to 70 cm through the ice growth period. The combination of oil and ice thicknesses, above and below the oil, presented a series of realistic oil detection scenarios. Table 1 provides the nominal ice and oil thicknesses used during the experiment. Overall, the combination of injections provided seven different experiments in which to quantify the detection of oil by sensors mounted above and below the sea ice.

Table 1. Injection conditions in primary hoops along the centerline. "A" hoops were injected on the same day as the primary hoop. Ice thickness was estimated from the distance to a sonar transducer plus an estimated freeboard height. The curvature of the ice bottom in Hoops 3-6 led to oil and ice thickness differences of several centimeters across the hoop.

Hoop ID	Injection Date & Start Time	Ice Thickness	Injection Amount	Sonar Measured Oil Thickness	Remarks
		cm	l	cm	
1	**5-Nov-14 16:37**	**5 - 15**	**90**	**1**	**Mix of broken ice and slush**
2	**12-Nov-14 13:39**	**16**	**150**	**1**	**Oil lost out one side of the hoop over a day**
3	**17-Nov-14 13:24**	**26**	**75**	**2**	
4	**20-Nov-14 12:45**	**29**	**225**	**4**	**Three injections over an hour to build oil slowly.**
1	**4-Dec-14 10:37**	**46**	**360**	**5**	
5	**9-Dec-14 11:40**	**54**	**150**	**6**	
6	**6-Jan-15 13:50**	**68**	**300**	**9**	

A detailed above- and below-ice sampling scheme was developed for each injection. Two primary measurement methodologies were used. "Point" measurements were collected by holding the carriages at a fixed location and collecting data with sensors capable of point data

collection. "Sweep" data was collected by activating the scanning sensors and performing a transect of the test basin, collecting data as the carriage was moving. A "hoop sweep" started at the center of the hoop prior to the one of interest, ran under the hoop of interest, and ended in the center of the hoop following the one of interest. For example, to perform a hoop sweep on Hoop 3, sensors would be activated in the middle of Hoop 2 and remain active while collecting data until the carriage reached the middle of Hoop 4. "Basin sweeps" were measurements made of the full length of the test tank.

Prior to the oil injection, a set of baseline measurements were made with all sensors above and below the ice. The aerial instruments were turned on and the above-ice carriage completed a baseline hoop sweep. A set of underwater instruments were turned on and a hoop sweep completed. Multiple underwater hoop sweeps with different sensors to operating were necessary to reduce instrument interference. After the hoop sweeps were complete, the underwater carriage was parked under the hoop to be injected to collect point measurements through the injection. The aerial sensors completed post injection hoop sweeps within an hour of the oil injection. Underwater sensors remained fixed below the injection site for an hour. After that the underwater instruments were cycled to allow all instruments to collect point measurements of the fresh oil, and hoop sweeps were conducted with all instruments. At the conclusion of the post injection hoop sweeps, the underwater carriage was parked under the hoop and a set of sensors monitored the oil over time until the next hoop or basin sweep was conducted.

Hoop sweeps were conducted with aerial and underwater sensors each day for the three days following each injection. Throughout the experiment, basin sweeps with all sensors were completed once a week. When not being used to make sweep measurements, the underwater

carriage and sensors were parked under the center of the hoop that had most recently been injected. When the scans with the aerial sensors were complete, the carriage and sensors were parked in the prep tank area that is isolated from the main tank allowing the equipment to be stored at 0°C

Detailed test ice properties were determined from ice cores and in-situ temperature probes. Temperature, salinity, density, ice texture and stratigraphy, and skeletal layer shape provided the information necessary for understanding sensor performance and as inputs into the subsequent modeling. Three-dimensional CT scans provided detailed information on brine and air inclusions, along with the ice microstructure of the boundary layer. This information was then used to provide experiment conditions for the modeling efforts.

After two months, when the ice reached its maximum thickness, the basin air temperature was raised to near 0°C and later raised further to accelerate ice melt. An artificial sun (high intensity lighting in the appropriate spectral band) was placed over one hoop and turned on for several hours a day for a week to examine how the simulated solar input changed the melt characteristics.

Oil-in-ice detection modeling was implemented to address a set of field scenarios based on two diameters of oil pools (2 and 200 m) and monthly ice growth. Specific ice parameters, such as temperature and salinity, were used to determine optical, acoustical, and radar properties of the ice in various situations and times of year. In addition, models also used the test-basin ice characteristics and the measured sensor performance in the laboratory for model validation.

RESULTS/DISCUSSION

Ice properties

Physical properties measured on ice cores during the experiment are representative of ice growth under natural conditions in the North American Arctic. Profiles of sea-ice salinity and temperature, as well as ice stratigraphy, were similar to with natural sea ice during mid-winter. CT scans were used to determine brine and air bubbles at high resolution. It also was used to follow the growth of the skeletal layer that was important to oil migration and acoustic measurements (Courville et al. 2017). A thin granular sea ice layer at the very top - less extensive than what is typically found under natural growth condition - transitioned into columnar texture persisting down the core, similar to Arctic sea ice.

Above-ice sensors

Our radar results were similar to those in previous tests. The ice-coupled (operated from the surface) GPR was able to detect both fresh and encapsulated oil throughout the ice growth. In addition, the airborne GPR was able to detect encapsulated oil when the ice was cold (Fig. 4). The FMCW airborne system being tested was a prototype and had difficulties in terms of reliability and noise in the data that are common with prototype devices. The results from the system were ambiguous, but modelling efforts suggest that FMCW has potential to detect oil in ice.

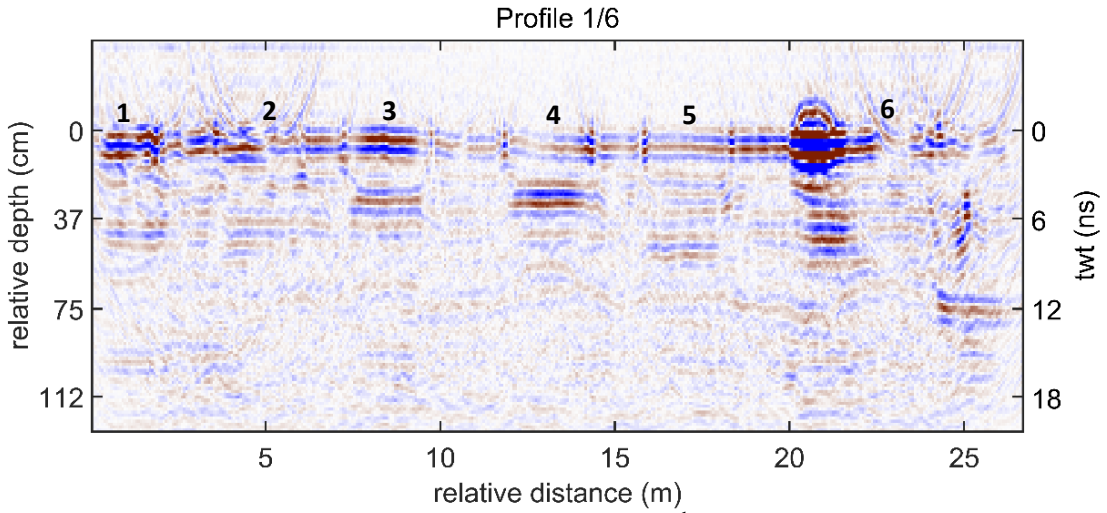

Figure 4. The aerial GPR full tank profile from January 6th, taken immediately prior to the injection into Hoop 6, shows the encapsulated oil in Hoops 3 and 4, with encapsulated oil also showing in Hoop 5. The mound at 21m is a pile of snow placed near the eastern edge of Hoop 6. The base of ice reflection is visible in most areas at a depth of 60-75 cm.

The optical sensors (cameras, radiometers, and fluorosensors) were able to detect oil at or very near the top of bare ice, but were not able to detect the oil through a thin layer of snow. These were the only technologies able to reliably detect oil in the frazil-brash ice mix from either above or below. The near-infrared spectra showed potential for discriminating oil from other dark targets. The thermal infrared sensors were also able to detect heating of oil at the surface of the ice.

Below-ice sensors

The presence of 1cm of oil blocked all light transmission through the ice (Fig. 5). The lack of light left it dark under the ice, thus allowing the oil to be detected using the cameras and radiometers even after ice grew below the oil. The model predicted that as ice grew under the oil that some light would fill in from the sides. The measurements confirmed this as the oil patches became less distinct over time, but still detectable. The fluorescence polarization sensor was able to detect oil through nearly six centimeters of ice below the oil (Fig. 6).

Figure 5. Still image of oil in hoop 5 looking from below.

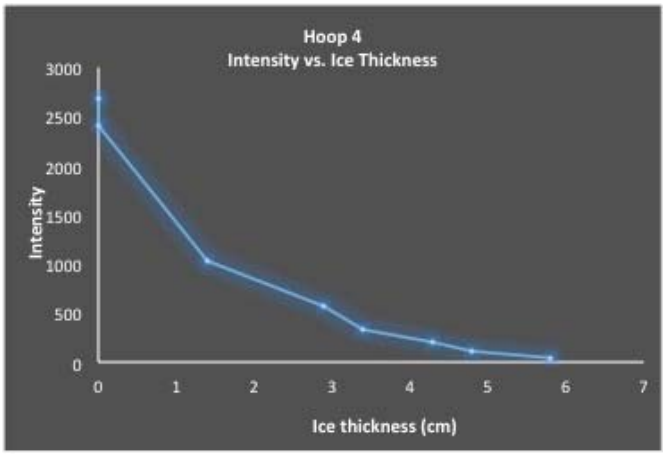

Figure 6. Plot of oil fluorescence intensity as a function of ice thickness.

Results from the narrowband, broadband, and nadir beams of the multibeam sonar units were similar. They were able to detect fresh oil under the ice, and the thickness of the oil could be determined (Fig. 7). Systems using frequencies in the 200 – 400 kHz range were able to detect oil through approximately six centimeters of new ice grown (Basset et al., 2016).

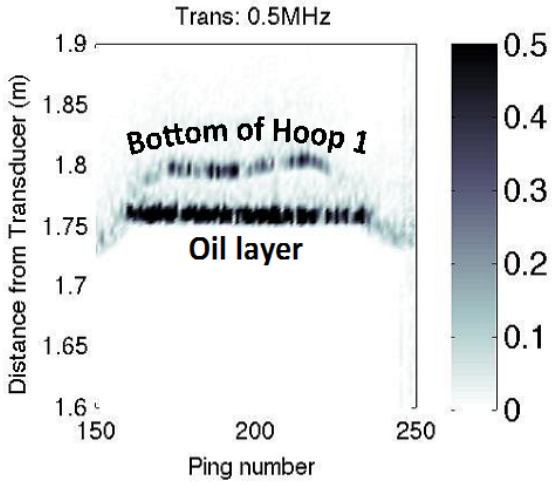

Figure 7. A transect under hoop 1 after an oil injection. The return from the base of the oil is the dark flat return, and the return from the ice is the lighter color above and to the sides of the oil.

Based on the results of the measurements and modeling efforts, the expected field performance of different sensors is provided in Table 2. Not surprisingly, the capability matrix shows that in pack or drift ice offshore, below-ice sensors are best at detecting fresh oil under the ice and existing airborne sensors are best at detecting oil on the surface or buried under snow. It is more difficult to detect oil encapsulated in the ice. The acoustics and fluorescence polarization sensors were able penetrate approximately 6 cm of new ice growth beneath the oil. The period during this new ice growth is expected to occur within a few days to a couple of weeks depending on the ice growth conditions.

There are limitations to the performance listed in Table 2. Passive optical sensors require sufficient light for observations. Their performance is also a function of the oil patch size, thickness of oil, and amount of ice below the oil. Similarly, thermal infrared sensors require enough sunlight to heat the oil in order to detect it. On-ice GPR measurements require a stable and safe ice surface to work on. Airborne radar systems will have difficulties in fall or spring

when the ice is generally too warm (high moisture content) and conductive. All the performance estimates are for level first-year ice.

Table 2. The expected field performance in level first-year ice of instrumentation tested during this experiment, based on laboratory and modeling results. Sensors include Ground Penetrating Radar (GPR), Frequency Modulated Continuous Wave Radar (FMCW), Optical (cameras and radiometers), Fluorescence Polarization (FP), Thermal Infrared (IR), and Acoustic systems. The P (for possible) rating indicates that there are conditions that may allow the system to work, and others when it is expected to fail. A yellow P2 rating indicates that there is still insufficient data fully assess performance. N/A indicates that sensor application in this scenario is not relevant – e.g. using below ice sensors to detect exposed oil on the surface.

Location	**Airborne**					**On ice**	**Below ice**		
Sensor	GPR	FMCW	Optical	FP	IR	GPR	Optical	FP	Acoustic
Fall-Winter-Spring									
Exposed oil on ice	Y	P2	Y	Y	P2	Y	P2	N/A	N/A
Snow covered oil on ice	Y	P2	N	N	N	Y	P2	N	N
Fresh oil under ice or with up to 6 cm encapsulation)	P2	P2	N	N	N	Y	Y	Y	Y
Encapsulated oil (more than 6 cm new growth)	P	P2	N	N	N	Y	P	N	P2
Summer									
Exposed oil on ice	P2	P2	Y	Y	Y	N/A	N/A	N/A	N/A

While this project represents an important start in evaluating sensor performance, further research is needed to take the results obtained in a controlled test basin and apply them to realistic field situations. For the most mature sensors it is important to conduct blind tests where the operators are unaware of the oil location. Systems, such as the FMCW, that remain at the prototype stage will require additional development and testing to determine their full

capabilities. The sonar systems were not able to transmit at full power in the test tank and may perform better in a natural environment.

The work here focused on sensor performance in bare, flat, first-year ice. An examination of rubble ice and other rough ice situations commonly found in nature would provide complimentary data to this study, and further challenge the sensors. Our laboratory testing capabilities are reaching their limits; to fully understand the capabilities and limitations of the various technologies in a realistic operational setting we need to plan, permit, and execute deliberate oil releases in the field.

CONCLUSIONS

This experiment provided an opportunity to test the capabilities of a wide range of above- and below-ice sensors to detect the presence of oil in a controlled environment. All sensor types used during this experiment showed an ability to detect oil on, in, or below ice under certain conditions. The results using above-ice sensors confirmed previous findings. The ability to detect fresh oil with acoustics was also confirmed. More importantly, this experiment demonstrated that acoustic and fluorescence polarization sensors could detect oil that had been encapsulated in ice up to six centimeters thick. The experiment also provided the first comparison of sensor performance for detecting oil in frazil and brash ice, an important scenario for the fall and spring transition seasons.

This project confirms the overall conclusion of previous work: that no one sensor has the capability of detecting oil in all situations. In addition, some sensors may complement each other in terms of oil thickness resolution vs. area coverage or swath width. Future operational

systems will likely employ suites of different sensors operating from various platforms under, on and above the ice surface to provide the means to detect oil in a range of ice environments at different times of the year.

Based on the results of this study, an effective underwater detection suite should have a low light camera, sonar, and possibly a spectral radiometer or fluorosensor. While the various sonar units had similar levels of performance, the multibeam type of sonar provides the added ability to create a 3D map of the underside of the ice that may help identify locations for oil to preferentially accumulate and narrow the search area (oil will naturally seek the highest spots in the under ice surface – thinnest ice regions).

The study results suggest that aerial sensors should include visible and thermal infrared imagers. Presently available radar technology provides the greatest potential for aerial mapping of oil on the ice surface or under snow, but requires future development to lead to an operational system. Ground penetrating radar operating from the ice surface is an appropriate tool as long as there is a stable and safe working environment.

REFERENCES

Bassett, C., A. C. Lavery, T. Maksym, and J. P. Wilkinson. 2016. Broadband acoustic backscatter from crude oil under laboratory-grown sea ice. *Journal of the Acoustical Society of America*. 140: 2274-2287. doi 10.1121/1.4963876.

Bradford, J.H., D. F. Dickins, and L. Liberty. 2008. Locating oil spills under sea ice using ground-penetrating radar. *The Leading Edge*. 27: 1424-1435.

Brown, C.E. 2011. Laser fluorosensors. In *Oil Spill Science and Technology: Prevention, Response, and Clean Up*. Edited by M. Fingas. Elsevier. Burlington, MA. USA. pp. 171-182.

Courville, Z.R., R. Lieb-Lappen, K. Claffey, B. Elder. 2017 Investigations of skeletal layer microstructure in the context of remote sensing of oil in sea ice. In Proceeding of the 2017 International Oil Spill Conference.

Dickins, D.F., J.H. Andersen, P.J. Brandvik, I. Singsaas, T. Buvik, J. Bradford, R. Hall, M. Babiker, K. Kloster, and S. Sandyen. 2010 Remote sensing for the Oil in Ice Joint Industry Program. In *Proceedings 33rd AMOP Technical Seminar*, Halifax, NS.

Dickins, D.F., H.P. Marshall, and R. Hay. 2012. Detecting oil in sea ice using Ground-penetrating radar: Developing a new airborne system. *2012 CRREL Test Report, prepared for Joint Industry Project Participants*. 30 pp.

Eguíluz, V. M., J. Fernandez-Gracia, X. Irigoien, and C. M. Duarte. 2016. A quantitative assessment of Arctic shipping in 2010–2014. *Scientific Reports.* 6: 30682; doi: 10.1038/srep30682.

Fingas, M. and C.E. Brown. 2013. Oil spill remote sensing. in *Earth System Monitoring,* edited by J. Orcutt. Springer. New York. pp. 337-388.

Maksym, T., H. Singh, C. Bassett, A. Lavery, L. Freitag, F. Sonnichsen, and J. Wilkinson. 2014. Oil spill detection and mapping under Arctic sea ice using autonomous underwater vehicles, *Final Report BSEE Contract E12PC00053.* U.S. DOI. BSEE. Washington, D.C., USA.99 pp.

Pegau, W. S., J. Garron, and L. Zabilansky. 2016. Detection of oil on-in-and-under ice, *Final Report 5.3*, Joint Industry Programme to define the state-of-the-art for surface remote sensing technologies to monitor oil under varying conditions of ice and visibility, London, U.K. 406 pp.

Puestow, T., L. Parsons, I. Zakharov, N. Cater, P. Bobby, M. Fuglem, G. Parr, A. Jayasiri, S. Warren, and G. Warbanski. 2013. Oil spill detection in low visibility and ice: surface remote sensing, *Final Report 5.1*, Joint Industry Programme to define the state-of-the-art for surface remote sensing technologies to monitor oil under varying conditions of ice and visibility, London, U.K. 82 pp.

Wilkinson, J., T. Maksym, and H. Singh. 2013. Capabilities for detection of oil spill under sea ice from autonomous underwater vehicles, *Final Report 5.2*, Joint Industry Programme on oil spill detection and mapping in low visibility and ice: focus on undersea remote sensing, London, U.K. 104 pp.